



ELSEVIER

Deep-Sea Research II 52 (2005) 73–88

DEEP-SEA RESEARCH
PART II

www.elsevier.com/locate/dsr2

Poleward and equatorward currents in the Pacific Eastern Boundary Current in summer 1995 and 1998 and their relationship to the distribution of euphausiids

Gordon Swartzman^{a,*}, Barbara Hickey^b, P. Michael Kosro^c, Chris Wilson^d

^a*Applied Physics Laboratory, School of Aquatic and Fisheries Science, University of Washington, Box 355640, Seattle, WA 98105-6698, USA*

^b*School of Oceanography, University of Washington, USA*

^c*College of Oceanographic and Atmospheric Sciences, Oregon State University, Corvallis, USA*

^d*National Marine Fisheries Service, Alaska Fisheries Science Center, Seattle, WA, USA*

Accepted 26 September 2004
Available online 25 January 2005

Abstract

This paper examines the relationship between poleward and equatorward current patterns and the spatial distribution of euphausiids based on acoustic survey data collected in summer 1995 and 1998 in the California Current Ecosystem. Contiguous poleward (usually an undercurrent) and equatorward near-surface current core areas were identified by applying current velocity and distance thresholds along each survey transect. Both currents were pervasive along the coast, but poleward volume transport in both years was about an order of magnitude greater than the equatorward near-surface current volume transports. The poleward volume transport was higher in 1998 than in 1995, especially north of Cape Blanco. The poleward transport centroid was generally further offshore than the surface transport centroid, and was closer to the slope in 1998 than in 1995. The depth centroid of euphausiid patches was generally shallower than the depth centroid of the poleward volume transport centroids. The onshore–offshore location of euphausiid patches was significantly related to the location of the poleward transport centroids, although not in all regions. The patches were not related to the location of equatorward near-surface transport centroids.

Differences in the north–south euphausiid distribution were observed between 1995 and 1998. In 1995, there was a much higher abundance of euphausiids in the region immediately north of Cape Blanco, while in 1998, euphausiid abundance was high throughout the survey area. We hypothesize this difference to be in part a result of differences in current patterns between the 2 years and the manner in which currents interact with euphausiid diel migration.

© 2005 Elsevier Ltd. All rights reserved.

*Corresponding author. Tel.: +1 206 5435997; fax: +1 206 5433785.
E-mail address: gordie@apl.washington.edu (G. Swartzman).

1. Introduction

The California Current Ecosystem (CCE) supports a great abundance of euphausiids dominated by *Euphausia pacifica* and *Thysanoessa spinifera*. These two species also serve as the major food item for pelagic fish species, especially the gadoid, Pacific hake (*Merluccius productus*, Livingston and Bailey, 1985; Tanasichuk et al., 1991), which is the most abundant mesopelagic fish throughout the CCE during the summer (Dorn et al., 1999). These euphausiid populations are pervasive along the coast and exist in large patches or swarms, which begin near the coast and can extend up to 150 km offshore, well past the continental shelf-break zone (defined as the zone having a bottom depth between 200 and 800 m, Swartzman and Hickey, 2003). Euphausiids migrate on a diel basis likely because of heavy predation (De Robertis, 2002), moving up in the water column at dusk, presumably to have access to their plankton food sources (both phytoplankton and smaller zooplankton, Nakagawa, 2002) and down again near dawn.

The diel migration occurs in the presence of strong coastal currents. In general, over the shelf in summer, currents are equatorward (Strub et al., 1990). Over the slope, surface currents are equatorward, but the seasonal poleward California undercurrent dominates subsurface currents (Hickey, 1998). This undercurrent, a ubiquitous feature of Eastern Boundary systems, generally has a higher velocity core at depths of 200–300 m, just below the shelf break. The high-speed core is relatively narrow (10–20 km), with typical speeds of 10–20 cm s⁻¹ (Pierce et al., 2000).

The strength and persistence of these currents provide a challenge to diel migrating euphausiids, which maintain average swim speeds between 1 and 2 body lengths per second (1.8–3.5 cm s⁻¹; De Robertis et al., 2003) and therefore cannot maintain their position by swimming against the currents. Thus, they may be at risk of being swept out of the shelf-break zone or away from aggregations of their prey. However, it has been suggested (Mackas et al., 1997) that adult euphausiids can maintain their position along the continental shelf break through diel migration.

Both the poleward undercurrent and the near-surface equatorward current, meander and change in velocity and size over space (Pierce et al., 2000). Thus, the effect of diel migration by euphausiids in the CCE on their spatial distribution may depend on both the longer-term pattern of the undercurrent and surface current and the onshore–offshore currents associated with upwelling and with tides. This paper examines the meso-scale pattern of these currents during summer 1995 and 1998 in the CCE and their relationship to euphausiid abundance to determine how the strength and location of the undercurrent and surface current influence the euphausiids' distribution.

2. Data and methods

The data used in this paper were collected by the National Marine Fisheries Service Alaska Fisheries Science Center aboard the M/S Miller Freeman during July and August 1995 and 1998. The ship was equipped with a hull-mounted (9-m depth) SIMRAD EK-500 split-beam echosounder operating at 38 and 120 kHz. An RD Instruments 153.6 kHz narrow-band, hull-mounted Acoustic Doppler Current Profiler (ADCP) measured currents throughout the survey. These data were processed, using University of Hawaii CODAS software, to produce north–south and east–west current velocities in 2.5-min horizontal (about 0.75 km at 10 knots) × 8-m vertical bins (Pierce et al., 2000; Kosro et al., 2001). The ship followed transects in an east–west direction, crossing the shelf-break zone at 10 nm intervals in both years from mid-California to Vancouver Island, British Columbia (Fig. 1, Swartzman and Hickey, 2003). Since the primary purpose of the survey, i.e. assessment of abundance of Pacific hake (*Merluccius productus*) was conducted during the daytime only, the majority of the data were collected during the day. For the present paper, only daytime data were selected.

Zooplankton patches were identified using both the 38 and 120 kHz data from SIMRAD, by image thresholds and by image differencing and morphological filters, based on geometric models and net corroboration (Stanton and Chu, 2000;

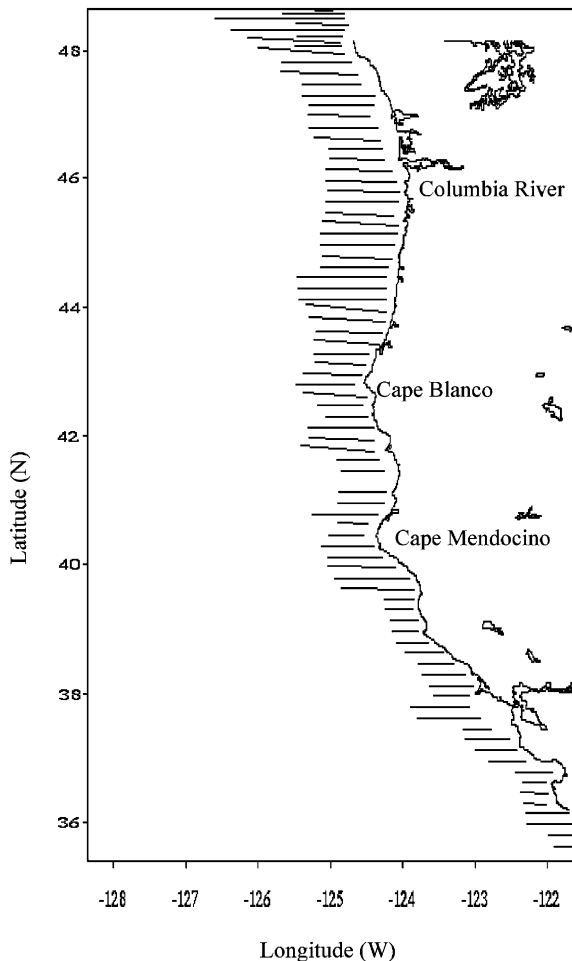


Fig. 1. Map of the acoustic survey area showing the transects followed in 1995 and the locations of the boundaries between the regions at Cape Mendocino, Cape Blanco and the Columbia River. Similar transects were surveyed in 1998.

Swartzman et al., 1999), making use of the fact that euphausiids, the dominant zooplankton in the pelagic zone of the CCE (Swartzman and Hickey, 2003; Swartzman, 2001), have higher backscatter at 120 kHz than at 38 kHz while fish do not (Swartzman and Hickey, 2003). The plankton patches identified were labeled using a connected component algorithm (Haralick and Shapiro, 1992), a method that puts numerical labels on each zooplankton patch (contiguous pixels identified in the images as being zooplankton), to allow further summary information to be made on an

individual patch basis. A suite of attributes was stored for each patch including location, size and shape, acoustic backscatter (acoustic biomass) and environmental parameters (e.g., bottom depth under the patch). The acoustic biomass index used throughout this paper is proportional to the zooplankton biomass but is not the actual biomass because no assumption has been made about euphausiid target strength or length distribution to convert to a true biomass estimate. Since the same algorithm is used throughout and the echosounder was identically calibrated in both years (Swartzman and Hickey, 2003), relative biomass can be compared between years and between locations.

A visual inspection of the plotted transect by transect ADCP data for 1995 and from the same survey in 1998, suggests that there was an almost ubiquitous poleward undercurrent and equatorward near-surface current in both years (e.g., Fig. 2). However, the locations and strength of these currents varied both in onshore–offshore location and depth range (Fig. 2). On some transects, there was more than a single poleward or equatorward velocity (e.g., 1998 transect at latitude 39.97 in Fig. 2) and poleward currents occasionally were observed in surface layers. The following algorithm was used to define the locations of the equatorward near-surface and poleward currents on each transect:

1. The east–west and north–south currents provided by the ADCP were resolved into onshore–offshore and poleward–equatorward components by identifying the direction of the 200-m isobath and resolving the currents into components along and perpendicular to this direction. Only the along-isobath components are used in the present analysis. Observed along-isobath currents are generally larger than typical along-isobath internal or barotropic tidal currents ($< 5 \text{ cm s}^{-1}$) over the West coast shelf and slope (Torgrimson and Hickey, 1979; Rosenfeld, 1990).
2. The ADCP poleward–equatorward velocity transects were used to locate (a) all areas having poleward flow greater than 7 cm s^{-1} , and (b) all areas having equatorward flow greater than

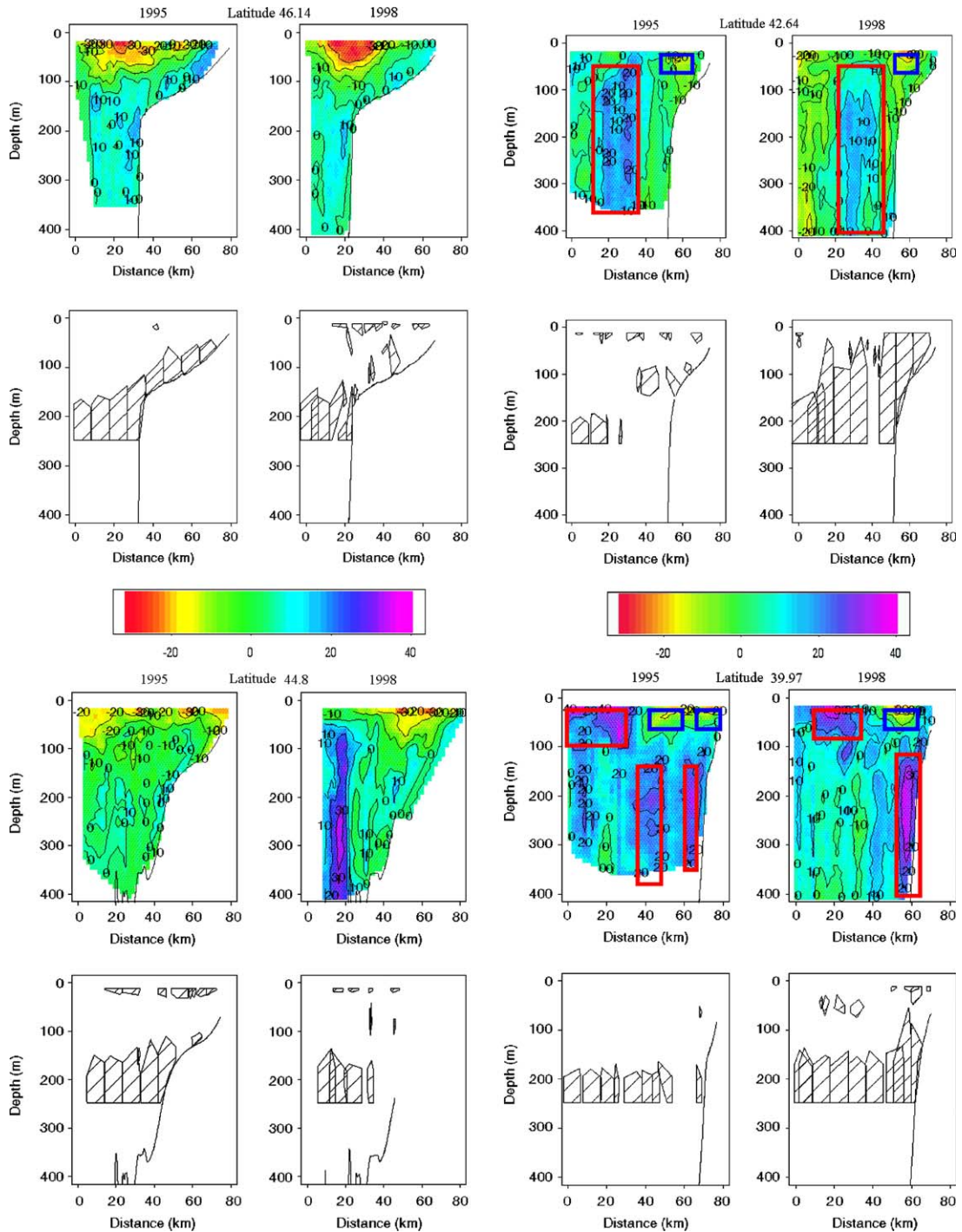


Fig. 2. ADCP velocity fields showing north-south velocity components of the current for replicate transects (i.e. transects at the same latitude) in 1995 and 1998 between 39.97°N and 46.14°N. The velocity scale is in cm s^{-1} . Bottom depths are shown on each plot and delineate the shelf and shelf-break zones of each transect. Locations of the poleward and equatorward core currents resulting from our algorithm are shown on selected panels by red (poleward) and blue (equatorward) rectangles overlaid on the ADCP velocity fields. Euphausiid patches are shown by diagonally shaded polygons on panels below the ADCP velocity fields for the same transect. The euphausiid data are limited to the top 250-m of the water column because of the resolution of the 120 kHz echosounder.

7 cm s^{-1} and a depth less than 100-m. ADCP data bins are 0.75-km horizontal \times 8-m vertical resolution. The flow thresholds were chosen to isolate areas having poleward or equatorward flow more than twice the maximum observed swimming speed of *Euphausia pacifica* (3.5 cm s^{-1} , De Robertis et al., 2003). A 100-m threshold was chosen for equatorward flow to assure that the algorithm located surface currents, based on the observation that the average boundary between poleward and equatorward flow in the CCE is \sim 100-m (Hickey, 1979). We did, however, allow the algorithm to locate near-surface poleward currents (e.g., Fig. 2 shows a poleward surface-trapped current along the 39.97°N latitude transect in 1998). This procedure could mistake a subsurface eddy for a meandering undercurrent because it discards the equatorward limb of any subsurface eddy if it lies below 100 m, but includes the poleward part.

3. Each velocity bin has a depth, latitude and longitude, representing its midpoint. To locate regions of high-velocity currents (separately for poleward and equatorward currents), we chose a distance threshold of 3-km. Adjacent areas left after the thresholding in step 1, having a gap between them greater than the threshold distance, were separated into two separate currents. This step identified groups of adjacent bins having high poleward or equatorward velocities. The choice of a 3-km distance threshold was based on the fact that empirical observations of the ADCP transect sections (Fig. 2) suggest that at least three intermediate bin widths (horizontal) must exist between contiguous high-velocity areas to define a separate current region. Volume transport was calculated for each delineated region by multiplying bin area by velocity in that bin.
4. For each delineated current region, we also calculated the centroids of longitude and depth (the centroid of longitude is the sum of the product of the longitude times the velocity of each bin in the current divided by the sum of all the velocities for bins in the current; the centroid of depth is calculated similarly from products of depth and velocity). When there

was more than a single poleward or surface equatorward current along a transect (as defined above), the region moving the largest volume of water per unit time (i.e. volume transport) was used to delineate the current location.

We chose this approach over the alternative of computing the centroid of all equatorward or poleward velocity areas greater than a threshold because (1) the examination of the ADCP data (Fig. 2) suggested the existence of distinct areas of higher poleward or equatorward velocity, and (2) when there is more than one such region, the overall centroid may not fall in an area of high velocity, thus misrepresenting the location of the region of strong transport. Nevertheless, we note that the centroid does not correspond to the location of the current's highest-velocity core if (1) it is computed across multiple cores, or (2) the currents around the core are not symmetrically distributed (e.g., an undercurrent with its maximum against the slope).

The centroid for the euphausiid distribution for each transect was calculated as the weighted average of the longitude of the centers of each euphausiid patch in that transect (the centroid is the sum of all patch center longitudes multiplied by patch acoustic biomass divided by the total euphausiid acoustic biomass for all patches in that transect). The 200 and 800-m isobaths were located, by interpolating and contouring bottom depth data from the 38 kHz echosounder system, to define the shelf (inshore of 200-m) shelf-break (between 200 and 800-m isobaths) and offshore zones.

To better illustrate the relationship between euphausiid centroids and volume transports, distances were calculated from the 200 and 800-m isobaths. We also plotted the distance of the centroid of the poleward current from the 200 and 800-m isobaths by transect against the respective distances from these isobaths of the equatorward surface current centroid and the centroid of the euphausiid acoustic biomass for each transect. Lastly, we calculated the correlation between these variables.

To further characterize regions, the coast was divided into four regions based on oceanographic and bathymetric properties (Thomas et al., 1994; Schwing et al., 2002; Swartzman and Hickey, 2003): (1) south of Cape Mendocino (termed South); (2) from Cape Mendocino to Cape Blanco (termed Blanco South); (3) from Cape Blanco to the Columbia River (termed Blanco North) and (4) from the Columbia River to the US–Canada border (termed North). Using these data, paired difference (paired by transect) *t*-tests were used to compare the poleward volume transport with the equatorward surface current volume transport in each region between years.

3. Results

3.1. Velocity and transport

A poleward flowing current, generally an “undercurrent” in the sense that the poleward flow has a subsurface maximum, was observed in both 1995 and 1998 (Fig. 2). The mean velocity of

the undercurrent ranged up to 26 cm s^{-1} and the mean surface current velocity ranged up to 39 cm s^{-1} (Fig. 3). No distinct latitudinal trend in equatorward surface velocities was observed. However, poleward velocities were a maximum in the South/Blanco South regions in both years and a minimum north of Cape Blanco, near $45\text{--}46^\circ\text{N}$. The difference between minimum and maximum poleward flow was about 5 cm s^{-1} . Mean poleward speeds were greater in the Blanco North region in 1995 than in 1998.

Along-coast and interannual differences in the strength of the poleward and surface currents are much more evident when the volume transport of water ($\text{m}^3 \text{ s}^{-1}$) is considered. The fact that both year-to-year and along-coast trends differ between velocities and volume transports indicates that the area over which the velocity acts has at least as much variability as the velocity itself. High poleward volume transport was evident south of Cape Blanco in both years (Fig. 4, Table 1). In 1998, high poleward volume transport also was observed in the Blanco North region; in 1995, the poleward volume transport in that region was much lower

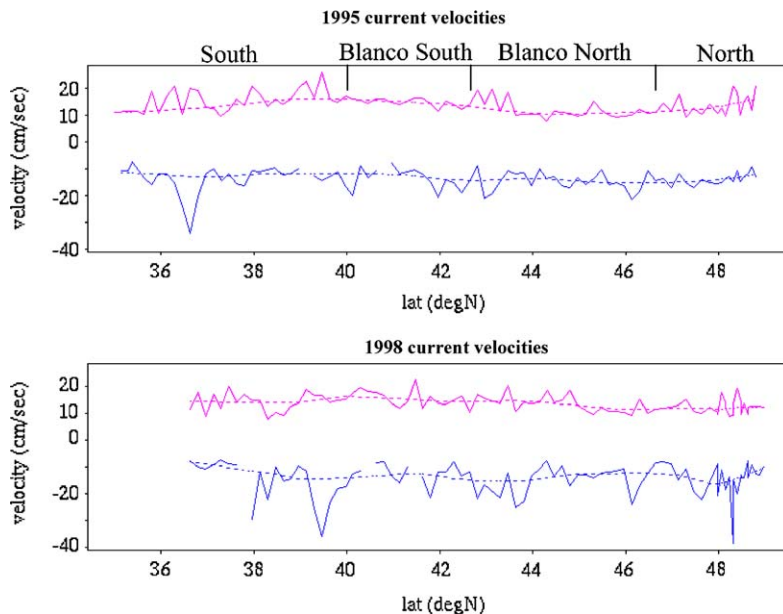


Fig. 3. Average speed (cm s^{-1}) of the largest poleward flowing regions (red) and equatorward flowing surface regions (blue, negative denotes equatorward flow) in each transect as a function of latitude for the 1995 and 1998 summer acoustic surveys. Dashed lines are smoothed currents using the lowest smoother, with filter window of $\frac{2}{3}$ of the data.

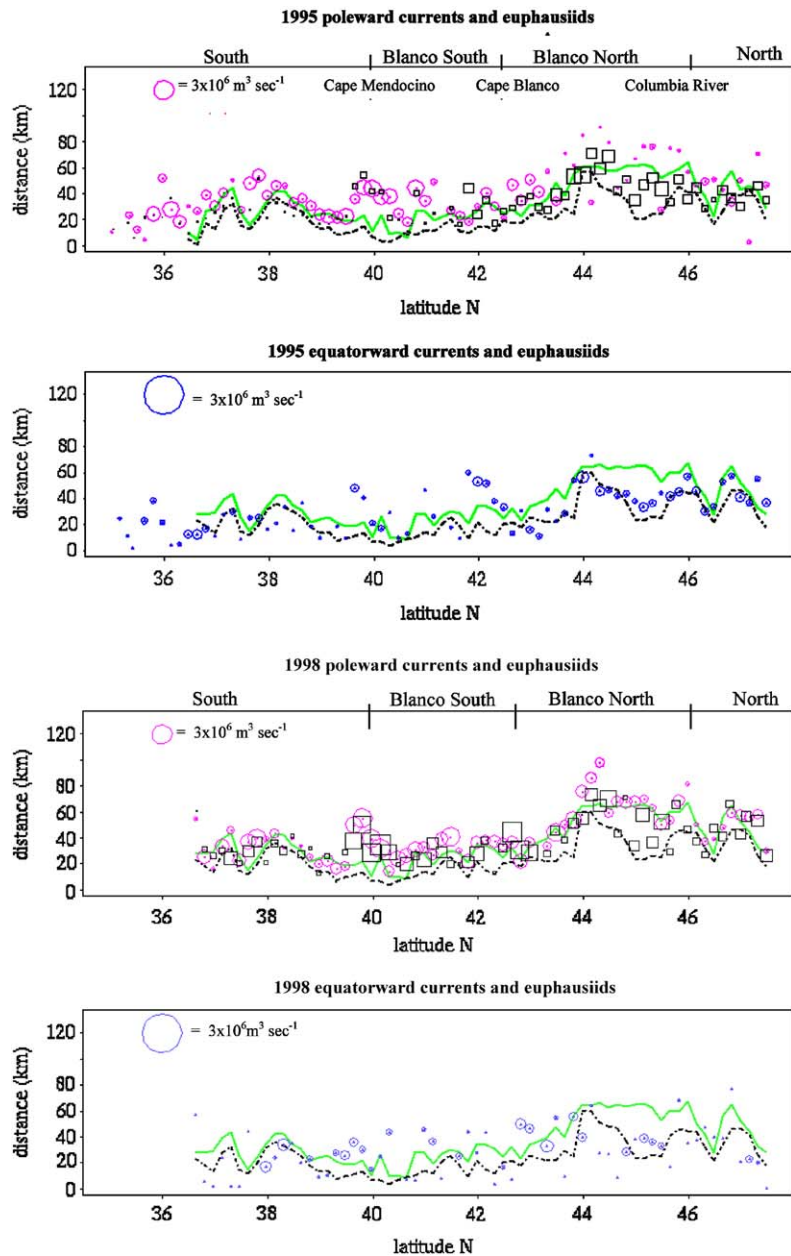


Fig. 4. Distribution and flow volume transport ($\text{m}^3 \text{s}^{-1}$) for 1995 (upper panels) and 1998 (lower panels) of the largest equatorward currents (blue) and poleward currents (magenta) in each transect shown by latitude and distance (km) from the coast along each transect. The volume transport circles are proportional in area to the current flow volume for that core current. There is a factor of two difference in scale between the equatorward volume transport and the poleward volume transport. Thus, the same-sized circle denotes twice the flow volume for poleward volume transport. The size and volume transport scales are the same for both years. Locations of the centroids of euphausiid distribution are shown by squares proportional in size to the total biomass for each transect. Green solid and black broken lines show locations of the 800 and 200-m isobaths, respectively.

Table 1

Poleward and equatorward (upper 100-m only) mean volume transport (in $10^5 \text{ m}^3 \text{ s}^{-1}$) and euphausiid acoustic biomass per transect in the region (1) south of Cape Blanco (South), (2) between Capes Blanco and Mendocino (Blanco South), (3) Cape Blanco to the Columbia River (Blanco North) and (4) north of the Columbia River (North) for the summer 1995 and 1998 cruises

Year/Region	South	Blanco South	Blanco North	North
1995 poleward	10.1 (1.1)	8.3 (1.48)	2.08 (0.73)	2.88 (0.38)
1998 poleward	11.0 (2.0)	13.4 (1.51)	8.94 (1.41)	3.68 (0.67)
1995 equatorward	-1.29 (0.26)	-1.37 (0.4)	-2.97 (0.47)	-2.31 (0.3)
1998 equatorward	-1.74 (0.52)	-1.17 (0.49)	-2.05 (0.59)	-0.73 (0.23)
1995 euphausiids	1.40 (0.24)	4.17 (0.60)	8.43 (0.51)	5.71 (0.72)
1998 euphausiids	7.12 (0.96)	8.64 (1.09)	8.46 (0.69)	7.25 (1.07)

Standard errors of the mean for each region are given in parentheses. A minus sign signifies equatorward flowing current.

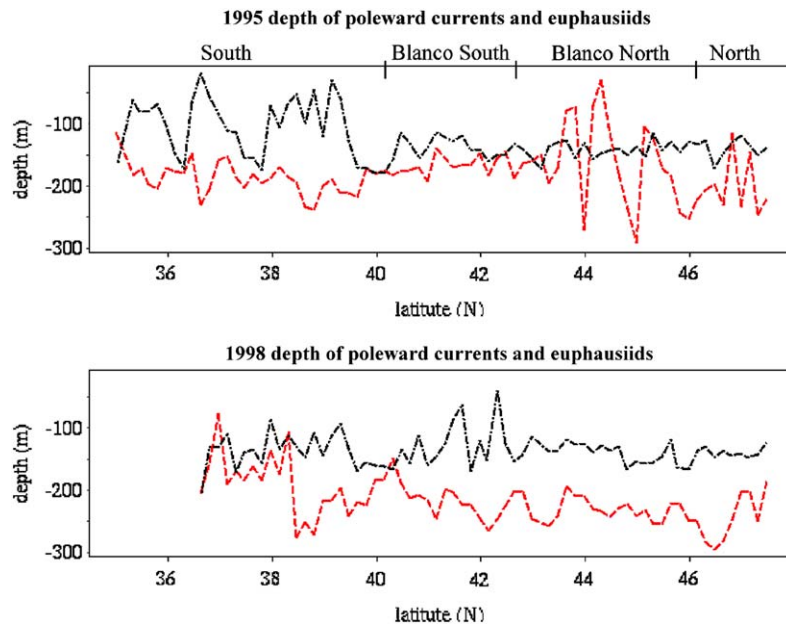


Fig. 5. Average depth of the maximum poleward volume transport (red) and euphausiid patches (black) for each survey transect in summer 1995 and 1998 as a function of latitude.

(Table 1). Statistical comparison (t -tests with degrees of freedom equal to the number of transects in each region minus 1) of the strength of the volume transport between the years showed that the poleward volume transport was significantly greater (level of significance for $\alpha = 0.05$, $p = 0-0.01$) in the region between the Columbia River and Cape Mendocino (i.e. Blanco South and Blanco North) in 1998 than in 1995, but not outside these regions, ($p = 0.17-0.35$). Surface

equatorward volume transport was greater in 1998 south of Cape Mendocino (South; $p < 0.05$, Table 1). Equatorward surface volume transport was approximately an order of magnitude less than poleward volume transport south of Cape Blanco, but ranged from 1:5 to 1:1 north of Cape Blanco (Table 1).

The depth distribution of the poleward volume transports differed over latitude between the 2 years (Fig. 5), particularly between 36°N and

44°N. Although the depth of the centroids for the poleward flow fluctuated, there was an apparent northward shoaling in 1995 in the depth of the poleward flow, from about 200-m at 36°N to 150-m at 44°N (see also Pierce et al., 2000). In 1998, the depth of the poleward transport deepened northward; from about 150-m at 36°N to about 250-m at 46°N. North of 44°N in 1995, the depth of the poleward flow was highly variable. In both years, the centroid of the region of poleward flow deepened north of Cape Blanco (Fig. 5).

Significant meandering of both the equatorward and poleward volume transports was observed, as suggested by the several tens of kilometer variability in the onshore–offshore locations of their centroids relative to the shelf break region (Figs. 4 and 6).

The location of the poleward transport centroid in both years was generally seaward of the shelf-break zone, while the surface current centroid was closer to shore, either seaward or shoreward of the

shelf-break (note x - and y -axis range in Fig. 6). Poleward centroids were typically located 0–35 km seaward of the 800-m isobath. However, in 1998, a preponderance of the centroids was within 10 km of the 800-m isobath (Fig. 6). The equatorward centroids also tended to be closer to shore in 1998 than in 1995. Only in the North and Blanco North regions and only in 1995 were any of the poleward centroids nearer shore than the 200-m isobath (i.e. on the shelf).

3.2. Euphausiid patch distributions

Like the velocity cores, the euphausiid patch abundance had different distributions in the 2 years (Fig. 4, Table 1). In 1995, euphausiid abundance was significantly higher in Blanco North ($p = 0$) compared to the other regions. In 1998, the distribution of euphausiids was more uniform along the coast (no significant difference between regions, see Fig. 4 and Table 1). In Blanco

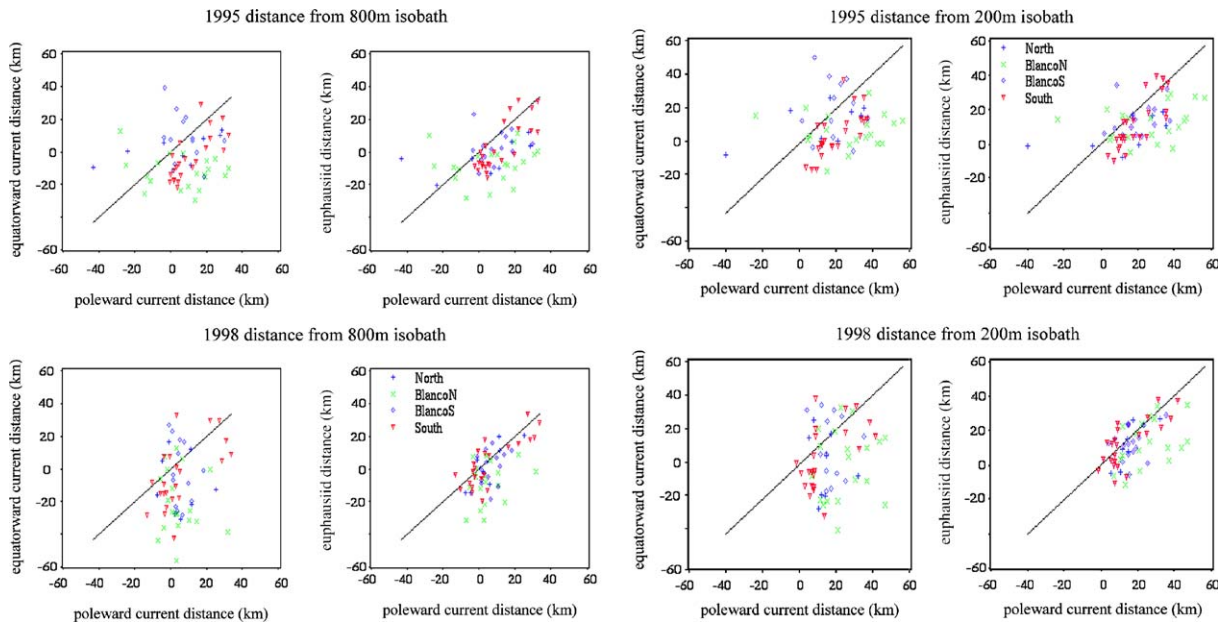


Fig. 6. Plots of the distance from the 800 (upper panels) and 200 m (lower panels) isobaths for the core poleward (primarily an undercurrent) volume centroid (x -axis) versus the distances (y -axis) of the equatorward surface current volume centroid (left panels, symbol and color coded by region) and the centroid of the euphausiid patches (right panels, symbol and color coded by region) for each survey transect in 1995 and 1998. Negative distance denotes distances shoreward of the isobath. Also shown on each plot are the line of equal distance. Points above the line have surface current or euphausiid centroid farther offshore than the poleward transport centroid, while the reverse is true for points below this line.

North, biomass was comparable in the 2 years; in the other three regions, biomass was higher in 1998 than in 1995. The interannual difference in euphausiid biomass and its relationship to current volume transport will be addressed with a simple transport model in Section 3.4 below. In general, patch centroids were frequently (but not always) found between the 200 and 800-m isobaths, and rarely found on the shelf (Figs. 4 and 6).

3.3. *Euphausiids and transport regions*

While the depth of the poleward transport centroid and euphausiid centroid each varied with latitude, the euphausiid centroid depth was generally shallower in the water column than that of the poleward transport (Fig. 5). In 1998, the euphausiid and transport centroids were separated by about 50–100-m or more over much of the coast.

A significant relationship was observed between the cross-shore positions of the centroids of the euphausiid patches and the poleward volume transports (i.e. close to the 1:1 line in Fig. 6), although the relationship did not hold in all regions or necessarily in both years. The euphausiid centroid was almost always nearer the poleward transport centroid than the surface current centroid (Fig. 6). The euphausiid centroids were also further onshore relative to the poleward transport centroids in 1995 than in 1998 (i.e. a higher proportion of euphausiid locations were below the 1:1 line in Fig. 6 in 1995 than in 1998). The fact that the onshore–offshore distribution of the poleward transport centroids was closer to the euphausiid centroid than the equatorward centroid is supported by correlations between them (e.g., for distances from the 200-m isobath, the correlations for 1995 and 1998, respectively, are $r = 0.17$ and 0.19 for poleward–equatorward centroid distances and $r = 0.48$ and 0.55 for poleward centroid–euphausiid centroid distance). However, these relationships vary from region to region. Only in the South and North regions is the relationship between distance from the 200-m isobath of the poleward transport centroid and the euphausiid core centroid significant in both years. From linear regression $r^2 = 0.48$

($p = 0.0002$) and $.37$ ($p = 0.001$) in the South and $r^2 = 0.61$ ($p = 0$) and $.76$ in the north ($p = 0$; accepting the alternative hypothesis that the slope is significantly greater than 0) for 1995 and 1998, respectively.

3.4. *Interannual biomass differences*

To explain the difference in the north–south euphausiid distribution between 1995 and 1998, we made a simple model of net transport north in each region. Using data shown in Fig. 3, we made the assumption that the average current speed in poleward undercurrent and equatorward surface current areas was 15 cm s^{-1} . Second, we assumed that there is no net poleward–equatorward transport for euphausiids outside these core currents. To ascertain what fraction of the euphausiids are in the core undercurrent and surface current cores, we assumed that the average breadth of both core surface and undercurrents was 15 km and that the average onshore–offshore region spanned by euphausiids was 40 km (Fig. 2, Swartzman and Hickey, 2003). This gives a $\frac{3}{8}$ average probability for the euphausiids to contact the core flows, assuming the euphausiids are uniformly distributed within their onshore–offshore range. To account for region-to-region and year-to-year differences in volume transport, we modified the probability of encountering a core current in each region by multiplying the average probability by the ratio of the volume transport in each region and year, to the average volume transport for both years over all regions (i.e. the mean overall undercurrent volume transport for undercurrent calculations and the mean overall surface current volume transport for surface current calculations, Table 1). Finally, we accounted for diel migration by assuming that by day (15 h), the euphausiids are deep and will be in potential contact with the poleward flowing undercurrent, while during the night (9 h), they will be in potential contact with the equatorward flowing surface current. Thus, we computed net daily transport by taking the difference of the undercurrent transport poleward and the surface current transport equatorward. Each is the product of average current velocity (15 cm/s for both currents,

Fig. 3) times the probability of contact ($\frac{3}{8}$), adjusted by region and year core volume transport ratio, times the number of hours in the undercurrent depths (assumed 15 h) or the surface current depths (9 h).

Calculated model results for net transport poleward for each year and region are given in Table 3. The estimated transports are surprisingly small, confirming that diel migration through a system of currents in opposing directions could provide an effective mechanism for reducing along-coast advection. The aggregation of euphausiid biomass around Cape Blanco in both 1995 and 1998 are consistent with the convergence of euphausiid transport toward Cape Blanco in both years (Table 3). The more uniform distribution in 1998 between Blanco South and Blanco North may be explained by the presence of northward euphausiid transport in Blanco North during 1998, compared to southward transport there during 1995.

4. Discussion

A dominant feature of the currents in both 1995 and 1998 was a spatially near-continuous poleward flow (typically an undercurrent) having average speeds of 10–20 cm s⁻¹ and volume transports usually greater than 1.0 × 10⁶ m³ s⁻¹. Equatorward surface currents were also ubiquitous. These upper-ocean currents had locally higher average velocities (i.e. > 20 cm s⁻¹), but generally lower volume transports (i.e. < 2.0 × 10⁵ m³ s⁻¹, Figs. 3 and 4, Table 1) than the deeper poleward currents.

The following discussion assumes that the differences between the 1995 and 1998 surveys are indicative of long-term differences. A shift to a cooler regime apparently occurred during 1998 (Schwing et al., 2002; Chavez et al., 2003). The 1995 survey occurred during a warmer regime, a regime with less than average upwelling winds in summer (Chavez et al., 2003). The 1998 survey was conducted during a transition period between a strong El Niño of 1997–1998 and a strong La Niña of 1998–1999. The more poleward distribution of Pacific hake (*Merluccius productus*, Swartzman and Hickey, 2003) is consistent with the stronger

poleward volume transport in 1998. Also, upwelling was stronger in these regions in 1998 than in 1995 (not shown here; Schwing et al., 2002; Swartzman and Hickey, 2003).

How do the current differences between the two years relate to the mesoscale north–south distribution and abundance of euphausiids? In 1995, there was a much higher abundance of euphausiids north of Cape Blanco (particularly in Blanco North), while in 1998, euphausiid abundance was high throughout the survey area (Table 1). Net euphausiid transport poleward may occur because diel migrating euphausiids spend much of the long summer days at depths dominated by the poleward undercurrent, moving into the equatorward flowing surface layer at night (Pillar et al., 1989). This hypothesis is supported by our simple model, which suggested net transport of euphausiids poleward in both years south of Cape Blanco, but only in 1998 north of Cape Blanco. Results from the NMFS survey and surveys by the Pacific Biological Station in Nanaimo, British Columbia, showed that euphausiid abundance was also high, north of the study area (within Canada) in 1998 (Ken Cooke, Pacific Biological Station, personal communication), consistent with significant north euphausiid transport. This information also suggests possible enhanced growth and reduced grazing pressure in northern regions in 1998. Stronger upwelling in the South and Blanco North regions in 1998 compared with 1995 may have provided enhanced feeding conditions for euphausiids (Swartzman and Hickey, 2003). We suggest that (1) net poleward transport all along the coast, (2) patchy but strong upwelling conditions, and (3) a more poleward distribution of Pacific hake and resultant reduced predation south of Cape Blanco (Swartzman and Hickey, 2003) resulted in high euphausiid levels throughout the CCE in summer 1998. In that year, high polewards euphausiid production and transport may have overcome hake predation pressure in the north to produce high euphausiid abundances. In contrast, the relatively lower upwelling in 1995 (Swartzman and Hickey, 2003) did not likely result in especially good euphausiid feeding conditions. Reduced upwelling, net poleward transport of euphausiids from south to north of Cape Blanco and high hake

abundance in the south may all have contributed to shaping the 1995 euphausiid mesoscale distribution pattern of reduced concentrations south of Cape Blanco (Swartzman and Hickey, 2003).

Our observations showed that, with few exceptions, patches of euphausiids were located 0–40 km seaward of the shelf break, and frequently between the 200 and 800-m isobaths. In 1998, the patches were predominantly within ~10-km of the 800-m isobath. Patch locations were statistically related to the onshore–offshore location of the poleward transport and the patch centroid was located typically shoreward of the centroid of poleward transport. Mackas et al. (1997), reporting on results of acoustic surveys in 1988 and 1991 over Nitinat Canyon British Columbia, suggested that euphausiids were locally aggregated along the shelf break in regions where the average velocity field converged toward the shelf break from offshore (i.e. the velocity was upslope toward the local bottom contours, following the slope of the upwelling isopycnals). They postulated a model for euphausiid transport, which relates to euphausiid diel migration as well as upwelling. They argued that the aggregation of euphausiids near the shelf break zone allowed them, through diel migration, to minimize equatorward transport in surface waters or even have net poleward transport by daytime transport north in the undercurrent. Support for the local aggregation hypothesis is also provided by Lu et al. (2003) in 1997–1998 studies off Western Vancouver Island British Columbia and Simard and Lavoie (1999) in studies in the Gulf of St. Lawrence, Quebec. For this model to be generally applicable, the upwelling zone must have a fairly extensive along-coast range, which, given the synchrony of current patterns from moorings at different points in the CCE during the summer, is often the case (Hickey and Banas, 2003). Thus, high production in the shelf and shelf-break zones should obtain over a large latitudinal range in association with large-scale upwelling events.

Our observations demonstrated that the onshore–offshore locations of both euphausiid patches and uni-directional current transport regions (both poleward and equatorward) have significant variability, typically within an envelope

~10–40 km from the 800-m isobath. Some of the variability in transport centroid location may be due to meandering of the high-speed undercurrent core that is typically located over the upper slope. Meandering and possible eddy formation in the poleward undercurrent (Pierce et al., 2000) may occur as a result of the current encountering Cape Mendocino and the wider shelf region to the north. This could produce meanders as well as eddies in the undercurrent by a method similar to the spawning of surface-trapped jets and eddies offshore when they encounter wind-driven surface currents with Cape Blanco (Strub et al., 1990; Hickey, 1998). When acoustically tracked underwater floats were released into the California Undercurrent, meandering and anticyclonic eddies were observed (Garfield et al., 1999). Eddies originating in the undercurrent have been reported by Kosro et al. (1991), Huyer et al. (1998), Chereskin et al. (2000) and Kosro (2002).

The high poleward transport region was generally located within about 0–40 km seaward of the 200-m isobath (Figs. 4 and 6). Since euphausiid abundance was frequently highest in the shelf-break zone slightly closer to shore (Swartzman and Hickey, 2003, Fig. 4), depending on exactly where the undercurrent was relative to the shelf break, the majority of diel migrating euphausiids might or might not be inside a poleward flow area during the daytime. Nevertheless, a significant relationship between location of patches and location of poleward transport was observed, although the robustness of the relationship varied with year and with region. The equatorward currents, although more variable onshore to offshore, were usually centered shoreward of the poleward currents and were frequently located over the shelf (Table 2, Fig. 6). Not surprisingly, no significant relationship to euphausiid patch location was observed.

The widespread north–south and onshore–offshore euphausiid distribution and the spatially variable current patterns (Figs. 2, 4 and 6, Swartzman and Hickey, 2003) allowed for a wide variety of current conditions encountered by different euphausiid patches. Thus, different euphausiid patches would encounter a different mix of poleward and equatorward current velocities. Their net transport through diel migration would

Table 2

Significance levels for paired-difference *t*-tests (paired by transect) for 1995 and 1998 surveys comparing the distance offshore of the centroid of the poleward transport volume relative to the equatorward current transport volume, and the distance offshore of each of these currents to the locations of the 200 and 800 m isobaths defining the boundaries of the shelf-break region

Hypothesis/year	1995	1998
H ₀ : equatorward surface current offshore of poleward current	$p = 0.0024$	$p = 0$
H ₁ : equatorward current nearer shore than poleward current		
H ₀ : poleward current offshore of 800-m isobath	$p = 0.287$ (NS)	$p = 0.075$ (NS)
H ₁ : poleward current nearer shore than 800-m isobath		
H ₀ : poleward current nearer shore than 200-m isobath	$p = 0.0025$	$p = 0.012$
H ₁ : poleward current offshore of 200-m isobath		
H ₀ : equatorward surface current offshore of 800-m isobath	$p = 0.0002$	$p = 0$
H ₁ : equatorward current nearer shore than 800-m isobath		
H ₀ : equatorward current nearer shore than 200-m isobath	$p = 0.08$ (NS)	$p = 0.88$ (NS)
H ₁ : equatorward current offshore of 200-m isobath		

NS denotes not significant at $p = 0.1$.

be the ensemble average of a spatially and temporally dynamic system. This flexibility, while not resulting in an optimal response to favorable local conditions (i.e. ability to stay close to large food patches), might, in the long run, compensate for the uncertainty of where favorable conditions may occur. For example, during a cooler regime (after 1998) and during La Niña conditions, the higher primary production may produce higher overall euphausiid feeding rates, while during the warmer regime years (e.g., 1995), having a broad onshore–offshore distribution of euphausiids may help them to succeed in local pockets, where they may be locally aggregated by strong onshore currents (Mackas et al., 1997) or eddy-like canyon-mediated currents (Hickey, 1998).

The net or average transport resulting from the interaction of spatially pervasive euphausiids, via diel migration, with meandering and variable poleward and equatorward currents can only be surmised: a crude first estimate of such transport was provided in this paper (Table 3). We have noted that the average transport appeared rather small to account for differences in euphausiid distribution between the years. However, we have assumed a random relationship between the location of the euphausiid distribution and the poleward and equatorward currents, while we found, in fact, a positive association between the centroids of the euphausiid distribution and the

Table 3

Estimated euphausiid net transport poleward (km day^{-1}) based on the velocity and volume of equatorward surface currents and poleward currents and the diel migration pattern of the euphausiids

Year/Region	South	Blanco South	Blanco North	North
1995	2.69	1.87	−2.33	−1.31
1998	2.55	4.16	1.39	0.69

Negative sign means that calculated net transport is equatorward.

poleward flow (Fig. 6). As such, we would expect more transport poleward than predicted by this model. A more rigorous, less assumption ridden and undoubtedly fruitful approach to assessing the effect of diel migration on transport would be to simulate euphausiid diel migration overlaid on the tapestry of observed current patterns using an individual-based particle movement model similar to the copepod transport model of Batchelder et al. (2002), but with a realistic current field as determined by ADCP data.

5. Summary and conclusions

In this paper, we have used whole coast ADCP surveys and acoustic backscatter data to describe spatial patterns of euphausiid patches and

equatorward (surface, upper 100-m) and poleward (frequently undercurrents) currents as well as volume transports to determine whether the currents are in any way related to patch location. Velocity cores were estimated using a threshold of 7 cm s^{-1} to define contiguous regions of high flow. Data from these two large-scale surveys are partly aliased by unresolved high-frequency variations in the physical and biological fields, at time scales from internal waves to storm forcing. However, based on broad-scale analysis of these data, we conclude:

1. Poleward flow, frequently flowing beneath an equatorward surface current, was ubiquitous along the coast in both years.
 2. The depth of this poleward flow region typically varied between ~ 50 and 300 m. Latitudinal trends in depth were opposite in the two years. However, in general, deeper poleward flow occurred north of Cape Blanco in both years.
 3. The volume transport of these currents showed greater differences than flow itself, both along the coast and between years. Generally higher transports occurred in 1998 than in 1995, and transports were particularly weak north of Cape Blanco in 1995.
 4. The cross-shore location of the poleward volume transport exhibited significant spatial cross-shore variability (typically ± 20 -km) but was almost always seaward of the shelf break. The poleward transport occurred closer to the slope in 1998 than in 1995.
 5. Equatorward currents in the upper 100 m were also ubiquitous along the coast, and the flow magnitudes had no apparent latitudinal trends.
 6. Equatorward near-surface volume transports were generally located inshore of the usually deeper poleward flows and the onshore–offshore positions of the centroids of the opposing transport regions were not significantly related ($r = .17$ and $.19$ for 1995 and 1998, respectively). Equatorward currents were frequently located on the shelf.
- With respect to euphausiids and their relationship to current patterns the analysis demonstrated:
1. Euphausiid biomass was greater north of Cape Blanco (and particularly in the Blanco North region) in 1995, in contrast to the more uniform along coast distribution in 1998. The relatively large euphausiid abundance north of Cape Blanco in 1995 may be related in part to the weak poleward volume transport in 1995 at those latitudes.
 2. The euphausiid patches were generally shallower in the water column than the poleward current, with a 50–100-m depth difference over much of the coast in 1998.
 3. In the onshore–offshore direction, the euphausiid patches were closer to the centroid of the poleward transport than to the centroid of the equatorward surface current transport, suggesting possible greater influence of the poleward currents on net poleward–equatorward transport. The patches were frequently (but not always) between the 200 and 800-m isobaths and usually closer to shore than the poleward centroids.
 4. In 1998, both poleward flow and upwelling were elevated compared with 1995, consistent with both increased poleward transport of euphausiids and increased euphausiid production (better feeding conditions).
 5. Net poleward transport of euphausiids was estimated south of Cape Blanco in both years. However there was no net poleward transport of euphausiids in regions north of Cape Blanco in 1995. These results were obtained via a simple model where undercurrent and surface-current volume transports were combined with assumptions about the breadth of euphausiid onshore–offshore distribution and diel migration pattern.
 6. Due to spatial (or temporal) variability in location of both poleward and equatorward currents and the breadth of euphausiid onshore–offshore distribution, local transport of aggregations of euphausiids can be quite variable. We suggest that having a broad onshore–offshore distribution may allow euphausiids to extend their range in a highly variable environment, thus reducing risk of the whole population encountering poor feeding and high predation conditions.

Acknowledgments

We thank Steve Pierce for making the 1995 processed ADCP data available. We would like to thank Andreas Winter for critical reading and suggestions on the manuscript. This work is supported by the National Science Foundation under Grants 0000734 and 0000735 as part of the NEP GLOBEC project, and under ONR Grants N00014-98-0026. It is contribution number 439 of the US GLOBEC program.

References

- Batchelder, H.P., Edwards, C.A., Powell, T.M., 2002. Individual-based models of copepod populations in coastal upwelling regions: implications of physiologically and environmentally influenced diel vertical migration on demographic success and nearshore retention. *Progress in Oceanography* 53, 307–333.
- Chavez, F.P., Ryan, J., Lluch-Cota, S.E., Niquen, C.M., 2003. From anchovies to sardines and back: multidecadal change in the Pacific Ocean. *Science* 5604, 217–221.
- Chereskin, T.K., Morris, M.Y., Niiler, P.P., Kosro, P.M., Smith, R.L., Ramp, S.R., Collins, C.A., Musgrave, D.L., 2000. Spatial and temporal characteristics of the mesoscale circulation of the California Current from eddy-resolving moored measurement. *Journal of Geophysical Research* 105 (C1), 1245–1269.
- De Robertis, A., 2002. Size-dependent visual predation risk and the timing of vertical migration: an optimization model. *Limnology and Oceanography* 47 (4), 925–933.
- De Robertis, A., Schell, C., Jaffe, J.S., 2003. Acoustic observations of the swimming behavior of the euphausiid *Euphausia pacifica* Hansen. *ICES Journal of Marine Sciences* 60, 885–898.
- Dorn, M.W., Saunders, M.W., Wilson, C.D., Guttormsen, M.A., Cooke, K., Kieser, R., Wilkins, M.E., 1999. Status of the Coastal Pacific Hake/Whiting Stock in US and Canada in 1998. NMFS, Seattle, 102pp.
- Garfield, N., Collins, C.A., Paquette, R.G., Carter, E., 1999. Lagrangian exploration of the California undercurrent, 1992–95. *Journal of Physical Oceanography* 29 (4), 560–583.
- Haralick, R., Shapiro, L., 1992. *Computer and Robot Vision*, vol. 1. Addison-Wesley, Reading, MA, 672pp.
- Hickey, B.M., 1979. The California current system: hypotheses and facts. *Progress in Oceanography* 8, 191–279.
- Hickey, B.M., 1998. In: Robinson, A.R., Brink, K.H. (Eds.), *Coastal oceanography of western North America from the tip of Baja California to Vancouver Island in the Sea*. Wiley, New York, pp. 345–393.
- Hickey, B.M., Banas, N.S., 2003. Oceanography of the US Pacific Coastal ocean and estuaries with application to coastal ecology. *Estuaries* 26 (4B), 1010–1031.
- Huyer, A., Barth, J.A., Kosro, P.M., Shearman, R.K., Smith, R.L., 1998. Upper-ocean water mass characteristics of the California current, summer 1993. *Deep-Sea Research II* 45, 1411–1442.
- Kosro, P.M., 2002. A poleward jet and an equatorward undercurrent observed off Oregon and northern California, during the 1997–98 El Niño. *Progress in Oceanography* 54, 343–360.
- Kosro, P.M., Huyer, A., Ramp, S.R., Smith, R.L., Chavez, F.P., Cowles, T.J., Abbott, M.R., Strub, P.T., Barber, R.T., Jessen, P., Small, L.F., 1991. The structure of the transition zone between coastal waters and the open ocean off northern California, winter and spring, 1987. *Journal of Geophysical Research* 96 (C8), 14707–14730.
- Kosro, P.M., Wilson, C.D., Smith, R.L., 2001. ADCP measurements from the 1998 Triennial Survey: NOAA ship Miller Freeman cruise 9810, July–August 1998. Data Report 181, Ref. No. 2001-1. College of Oceanic and Atmospheric Sciences, Oregon State University, Corvallis, OR 97331-5503.
- Livingston, P.A., Bailey, K.M., 1985. Trophic role of Pacific whiting, *Merluccius productus*. *Marine Fisheries Review* 47 (2), 17–22.
- Lu, B., Mackas, D.L., Moore, D.F., 2003. Cross-shore separation of adult and juvenile euphausiids in a shelf-break alongshore current. *Progress in Oceanography* 57, 381–404.
- Mackas, D.L., Kieser, R., Saunders, M., Yelland, D.R., Brown, R.M., Moore, D.F., 1997. Aggregations of euphausiids and Pacific hake (*Merluccius productus*) along the outer continental shelf off Vancouver Island. *Canadian Journal of Fisheries and Aquatic Sciences* 54, 1–18.
- Nakagawa, Y., 2002. Feeding ecology of *Euphausia pacifica* Hansen in the northwestern North Pacific. Ph.D. Tohoku University. 114pp.
- Pierce, S.D., Smith, R.L., Kosro, P.M., Barth, J.A., Wilson, C.D., 2000. Continuity of the poleward undercurrent along the eastern boundary of the mid-latitude Pacific. *Deep-Sea Research II* 47, 811–829.
- Pillar, S.C., Armstrong, D.A., Hutchings, L., 1989. Vertical migration, dispersal and transport of *Euphausia lucens* in the southern Benguela Current. *Marine Ecology—Progress Series* 53, 179–190.
- Rosenfeld, L.K., 1990. Baroclinic semidiurnal tidal currents over the continental shelf off northern California. *Journal of Geophysical Research* 95 (C12), 22153–22172.
- Schwing, F.B., Murphree, T., DeWitt, L., Green, P.M., 2002. The evolution of oceanic and atmospheric anomalies in the northeast Pacific during the El Niño and La Niña events of 1995–2001. *Progress in Oceanography* 54, 459–491.
- Simard, Y., Lavoie, D., 1999. The rich krill aggregation of the Saguenay- St. Lawrence Marine Park: hydroacoustic and geostatistical biomass estimates, structure, variability and significance for whales. *Canadian Journal of Fisheries and Aquatic Sciences* 56 (7), 1182–1197.
- Stanton, T.K., Chu, D., 2000. Sound Review and recommendations for modeling of acoustic scattering by fluid-like

- elongated zooplankton: euphausiids and copepods. *ICES Journal of Marine Sciences* 57 (4), 793–807.
- Strub, P.T., James, C., Thomas, A.C., Abbott, M.R., 1990. Seasonal and non-seasonal variability of satellite derived surface pigment concentration in the California Current. *Journal of Geophysical Research* 95, 11501–11530.
- Swartzman, G.L., 2001. Spatial patterns of Pacific hake (*Merluccius productus*) shoals and euphausiid patches in the California Current Ecosystem. Lowell Wakefield Symposium on Spatial Processes and Management in Fisheries AK-SG-01-02 1, 495–512.
- Swartzman, G.L., Hickey, B., 2003. Evidence for a regime shift after the 1997–1998 El Niño, based on triennial acoustic surveys (1995–2001) in the Pacific Eastern Boundary Current. *Estuaries* 26 (4B), 1032–1043.
- Swartzman, G.L., Brodeur, R., Napp, J., Walsh, D., Hewitt, R., Demer, D., Hunt, G., Logerwell, L., 1999. Relating fish and plankton acoustically sampled at different frequencies: data viewing, image analysis and spatial proximity. *Canadian Journal of Fisheries and Aquatic Sciences* 56, 545–560.
- Tanasichuk, R.W., Ware, D.M., Shaw, W., McFarlane, G.A., 1991. Variations in diet, daily ration, and feeding periodicity of Pacific hake (*Merluccius productus*) and spiny dogfish (*Squalus acanthias*) off the lower west coast of Vancouver Island. *Canadian Journal of Fisheries and Aquatic Sciences* 48, 2118–2128.
- Thomas, A.C., Carr, M.E., Strub, P.T., 1994. Chlorophyll variability in eastern boundary currents. *Geophysical Research Letters* 28 (18), 3421–3424.
- Torgimson, G.M., Hickey, B.M., 1979. Barotropic and baroclinic tides over the continental slope and shelf off Oregon. *Journal of Geophysical Research* 9 (5), 945–961.